

A Displacement Based Design Approach For Seismic Assessment of Flat Slab Structure With Core Shear Wall

Khondaker Sakil Ahmed¹, Mohana Kawsher², Rezvi Ahmed³, Rishath Sabrin⁴, Samia Zakir Sarothi⁵, Afia Farzana⁶
^{1,2,3,4,5,6} Military Institute of Science and Technology
Mirpur Cantonment, Dhaka, Bangladesh
drksa@ce.mist.ac.bd; mohana.trisha313@gmail.com; rezvinayon97@gmail.com; s.rishath.ce12@ce.mist.ac.bd;
afia@ce.mist.ac.bd; zakirsamia@ce.mist.ac.bd

Abstract - Reinforced concrete (RC) structures containing flat slab system and core shear wall have become popular and have been used extensively all over the world for the last few decades. They provide substantial advantages over the traditional beam-column-slab structures in terms of architectural aesthetics, easier fixing of electrical, lift, and plumbing lines. Usually, the building system consists of an RC core shear wall and columns directly connected to the slabs. Though the design procedure is similar to the structural type consisting of moment frames, the existing force-based seismic design practice has some limitations in considering response modification factors, design overstrength, deflection amplification factors, ductility, etc. In this study, an 8-storey flat slab RC structure with core shear-wall and gravity columns is considered for non-linear dynamic analysis. The displacement-based design approach addressed six pairs of ground motions. The core wall was modelled as fiber hinge model where hysteretic responses of both concrete and steel fiber responses are investigated. The results are presented in terms of the storey response, base shear, and roof displacement of the structure. Column, wall, and fiber hinges responses highlight the states of individual components as well as the fibers. Finally, the stress and strain levels of concrete and steel fibers are examined to check the overall status of the structural system.

Keywords: RC structure, core shear wall, displacement-based analysis, dynamic time history analysis, hysteretic response.

1. Introduction

The conventional method of earthquake analysis accounts prescribed level of the lateral shear force hitting the structure in one dimensional way and it defines only one level of damage. The primary aim of the existing building design code is to provide life safety (strength and ductility), control damage (drift limits as serviceability) in minor and moderate earthquakes, and prevent collapse in a major earthquake. However, real earthquake propagates as wave and more than one damage level can emerge under one earthquake. The design criteria are based on stress limits and member forces calculated from prescribed levels of applied lateral shear force [1, 2]. The procedure may not guide the designers to address seismic events particularly for flat slab structures or structures with irregular geometry.

Generally, core wall systems are widely used in tall structures in a view to resisting the major amount of shear force by the wall and taking the higher flexural rigidity into account to reduce structural deflection [1]. Alternative approaches such as dampers and base isolators are also widely used to mitigate seismic forces on the structures [3-5]. However, ordinary frames such as structures with a flat slab or flat plate slab system may take the advantage of core shear wall expecting that they will take the major lateral forces and control the deflections. Therefore, the columns may experience a smaller shear force that can reduce the potential earthquake vulnerability.

Displacement base analysis is an established and more defined design procedure which is capable to estimate damage of any structure that may experience after the seismic event and hence identify its multiple performances and hazard levels [6]. Subsequently, performance-based seismic design is based on the displacement based design procedure where the stakeholders set different performance objectives for a structure for future earthquakes [7]. In a view to control damages, different repair and retrofitting technique [8] such as column or wall jacketing or post installed rebar or stainless steel reinforcements have already been established for structural strengthening [9, 10]. Performance objectives are operational (O), immediate occupancy (IO), life safety (LS), collapse prevention (CP), in which Life safety is the major focus to reduce the threats to the life safety of the structure. Damage to the RC wall may include steel reinforcement yielding or buckling,

fracture of concrete and permanent horizontal drift after a severe event. Generally, damages in RC walls due to the plasticity extension are difficult to repair. Besides, buildings with large residual drifts require expensive structural repair and will often be out of service for long periods.

This study aims to investigate the RC flat slab structure with core shear wall using displacement-based design approach. An 8-storey commercial building containing a core shear wall and gravity columns are considered. The response of the structure in terms of displacement, storey shear, drift is examined for seven different ground motions. The core wall is modelled as fiber hinges for both concrete and steel. This alternative analysis approach will also highlight those fiber hinge responses of core shear wall as well its contribution in the global response.

2. Finite Element Model of the Structure

A 3D finite element model of the RC structure with flat plate system containing columns and core shear wall has been developed using commercial building design software ETABS of CSI Inc. [11]. The plan view of the structure with dimensions is shown in Fig. 1. The basic dimensions are kept as 22 m in the x-direction, 22 m in the y-direction, 4.25 m of bottom story height and 3 m of typical floor height. Both geometric and material non-linearity are considered in the analysis procedure.

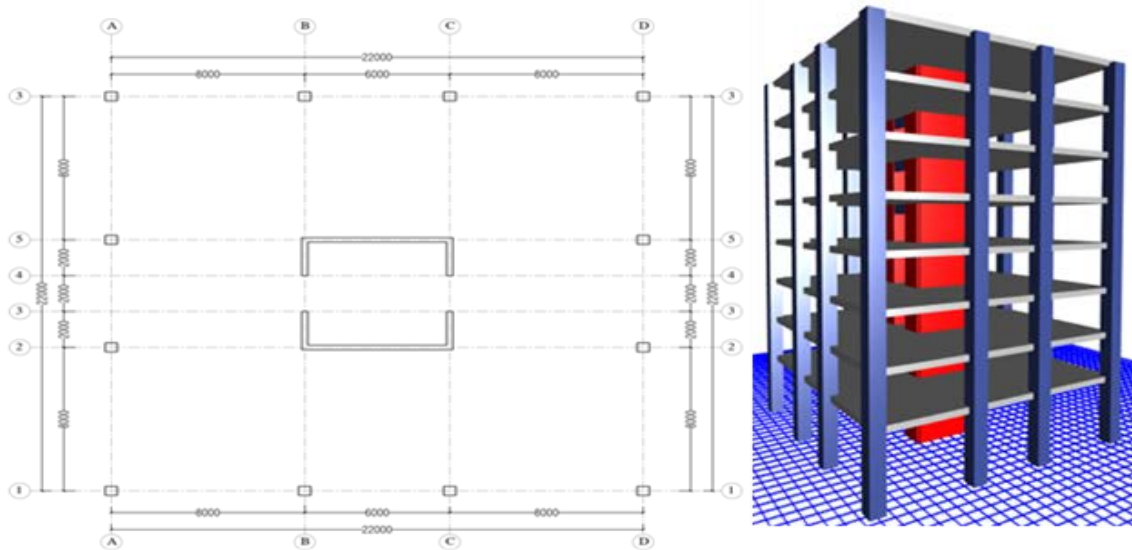


Fig. 1: Floor Plan and 3D Finite Element Model of Structure (all dimensions in mm)

2.1. Sectional and Material Properties

The size of all the column is 500×500 mm square. The dimension of the coupling beams are section of 250 mm×500 mm. The thickness of the core shear wall is 250 mm considering as reinforced concrete wall. All the column section was chosen same all over the building for simplification. The density of Concrete and brick walls are 24 kN/m³ and 20 N/m³ respectively. The slab thickness was kept uniform to be 200 mm for all floors as material properties, a standard 35 MPa concrete and 60-grade steel are used in the analysis process as shown in Table 1.

Table 1: Material Property

Material	Property	Values
Concrete	Compressive Strength (MPa)	35
	Modulus of Elasticity (GPa)	34
Steel Reinforcement	Yield Strength (MPa)	355
	Tensile Strength (MPa)	510
	Modulus of Elasticity (GPa)	21

The load patterns and combinations of the preliminary force-based analysis are presented on Table 2 and 3 respectively. The total weight of the building is (DL+ 25% of LL) is approximately 6000 tonnes. Other seismic design parameters are given in Table 4. Considering an OMRF (R=3 as per ASCE 7-10) at the Sylhet zone (Z=0.36g) and soil type E (ASCE 7) [12] of Bangladesh, the PMM ratio has been checked for the concrete columns before going into the non-linear analysis of the structure. The capacity of structural columns and shear wall was kept within the limit. The non-linear behavior of the material is presented in Fig. 2. The kinematic hardening model is considered for hysteretic responses of the rebar.

Table 2: Loads on typical floors and roof

Load Patterns	Descriptions	Roof
DL	1.5 kN/m ²	1.5 kN/m ²
LL	5 kN/m ²	2 kN/m ²
PW	5.5 kN/m ²	0.25 kN/m ²
UTILITY	1 kN/m ²	0 kN/m ²

Table 3: Selected Load Combinations

Combinations	Descriptions
1	1.4DL ^a
2	1.2DL+1.6LL ^b
3	1.0DL+1.0LL+1.0Ex ^c
4	1.0DL+1.0LL+1.0Ey ^d

^aDead Load; ^bLive Load; ^cEarthquake Load in x-Direction; ^dEarthquake Load in y-Direction

Table 4: Total masses and seismic design parameters

No. of Story	Loads	Total Mass (kN)	Seismic Design Parameter
8	DL	34186.66	S _s = 1 S ₁ = 0.3
	LL	17020	Site Class: C Risk Category: III
	PW	17825	SDC: E I= 1
	UTILITY	3220	R= 3, C _d = 3

Note: SDC = Seismic Design Category

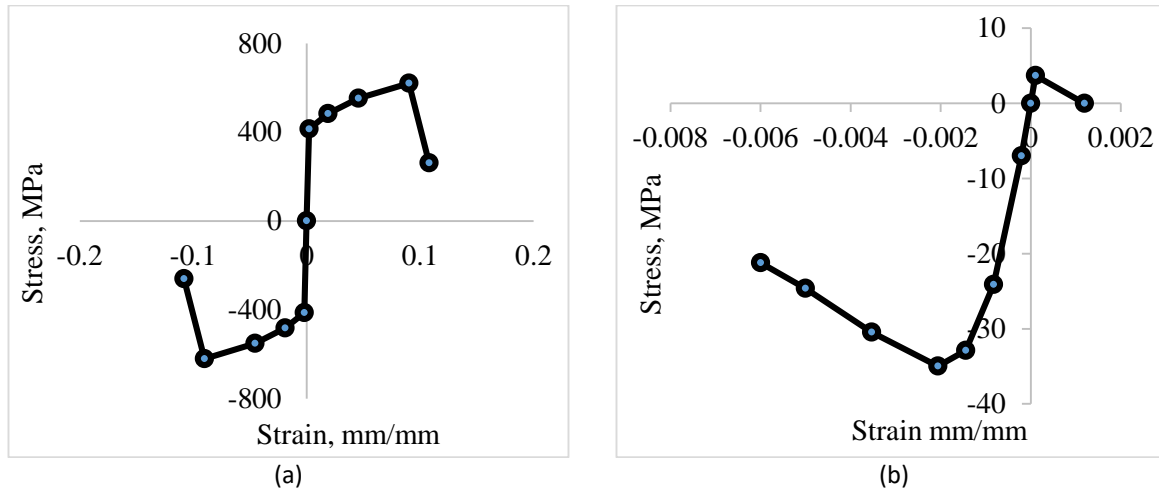


Fig. 2: Material non-linearity; (a) Steel and (b) Concrete.

The non-linear sectional properties in terms of moment-curvature relationship of column and shear wall are presented in Fig.3. It is a representation of bilinear moment curvature relationship in non-linear analysis. As the moment to capacity ratio increases the curves seem to fall as it cannot take much moment as the load increases that much after this failure will occur. In Figure, different moment curvature diagram of the section is given. The section cannot carry more moment than approximately 25000 kN-m. A section undergoes fiber to fiber redistribution when these moment values are reached. If the curvature of the element is greater than approximately 0.05 m^{-1} , the section capacity reduces to approximately 75 kN-m, in other words, plastic hinges are formed.

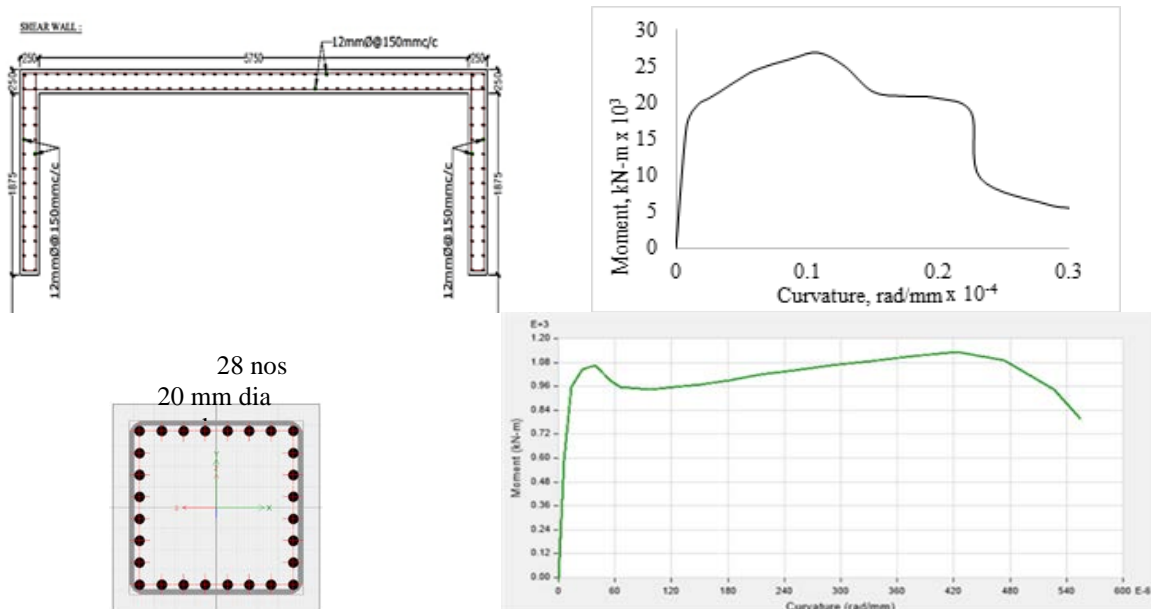


Fig. 3: Moment curvature relationship of shear wall and column section.

2.2. Hinge Properties

Beam and column elements were modeled as nonlinear frame elements with lumped plasticity by defining plastic hinges at both ends of beams and columns. In this study, user-defined hinge properties were implemented. The plastic hinge locations were assumed and defined on the two ends of the column and beam elements. The seismic performance

evaluation was carried out in accordance with FEMA 356 guidelines. For columns and walls, fiber hinges have been used as per ASCE as shown in Fig. 3. As an addition Shear behavior is usually not coupled with bending so it is desirable to maintain shear demand below shear capacity to ensure ductile flexural behavior is the governed action. For vertical and horizontal rebar percentage of the wall was used to be 1.1% and 0.27%, respectively. Fig. 4 presents the hinge properties and wall hinge fibers. Fig. 4(a) presents the fiber hinges; blue as steel fiber and gray as concrete fiber. Fig. 4(b), 4(c), and 4(d) present the strain limit at different performance objectives and the backbone curve of the nonlinear hinge behavior.

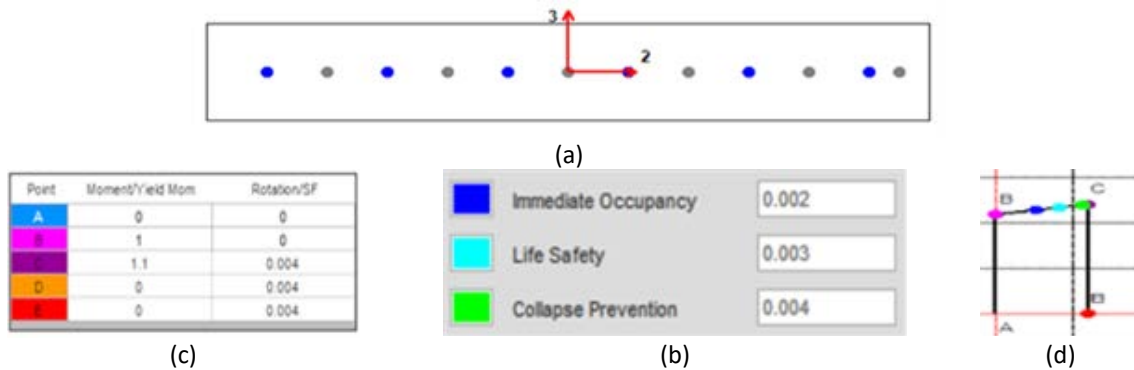


Fig. 4: Hinge Properties (a) Shear Wall (Fiber segments): Blue- Steel; Grey- Concrete; (b) Strain limit at different point; (c) IO, LS and CP strain levels; (d) backbone curve.

2.3. Ground Motions

The six pairs of ground motions (both X and Y Direction) are considered in this study as presented in Table 5. These are recorded earthquake and will be scaled to approximately 1.35g to represent an MCE earthquake. The peak displacement from NTH is not correspond to ultimate displacement from pushover analysis. For nonlinear analysis, FNA usually uses Ritz vector which is customized with P-Delta based on the gravity loads. It is important to use P-delta as it is critical in properly determining stability behavior.

Table 5: Earthquake GMs used in study

Serial No.	TH function	PGA (g)	Scale factor
1	Lacc_Nor-1	0.221	4.53
2	Lacc_Nor-2	0.255	3.91
3	Corralit-1	0.629	1.59
4	Corralit-2	0.477	2.09
5	Kobe-1	0.275	3.64
6	Kobe-2	0.324	3.09
7	Landers-1	0.723	1.38
8	Landers-2	0.779	1.28
9	Imperial Valley-1	0.353	2.83
10	Imperial Valley-2	0.482	2.07
11	Tabas-1	0.845	1.17
12	Tabas-2	0.856	1.16

3. Results and Discussions

The displacement-based design approach can determine the hinge states of structural components subjected to different ground motions. A typical hinge state of the structure under maximum considered earthquake is shown in Fig. 5. The color of the hinges indicates the hinge behavior and their status under the ground motions. For light green, the hinge is at or past collapse prevention this indicates the structural member may require a redesign. And shear walls are most vulnerable as it takes the maximum shear wall and prevents the building from collapse. The hinge outcome shows that some hinges of the walls are in red zone particularly at the ground to first storey zone indicating the larger hinge rotation occurs in the walls first. According to FEMA356, the reinforced-concrete shear-wall building is expected to satisfy LS performance levels under the design earthquake. It can be seen from the above figure that the building's structural members show a linear mode of failure for certain time period.

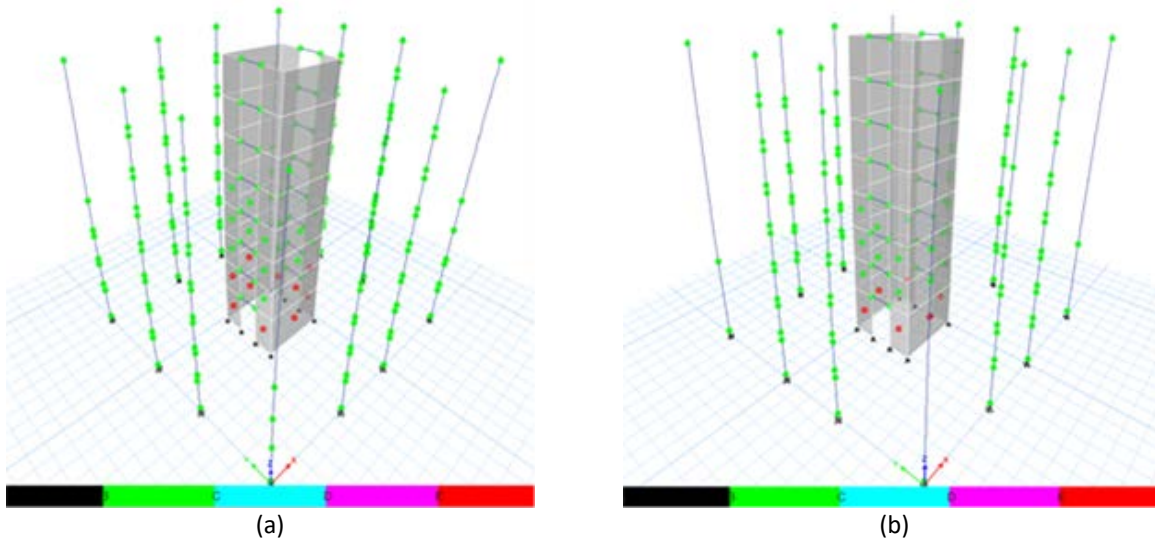


Fig. 5: Plastic hinges formation of the structure (a) Lacc_Nor and (b) Kobe earthquake.

Comparison of base shear is made between different time history functions as shown in Fig.6 and tabulated, in which it clearly shows that the base shear obtained from Lacc_Nor gives is considerably higher than resulting from others GMs. The storey shear forces for different ground motions are presented in Fig.7. The maximum storey shear in X and Y directions are found for Lacc_Nor and Corralit time histories, respectively. The maximum storey shear of core shear wall and combined all columns for different ground motions are presented in Table 6. It can be concluded from the result that all most 98% of the total shear force is carried by the core shear wall that left the columns to carry only 2%. The previous results also shows similar findings where shear wall is proposed to carry the shear generated from lateral forces [13].

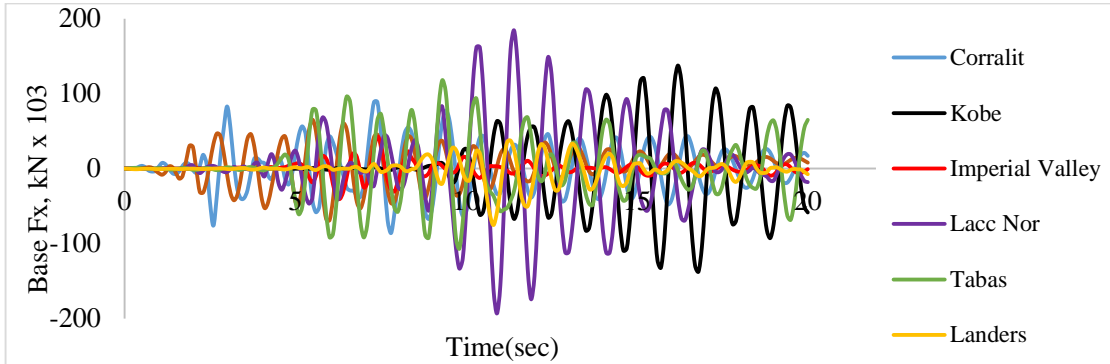


Fig. 6: Base shear under different earthquake GMs.

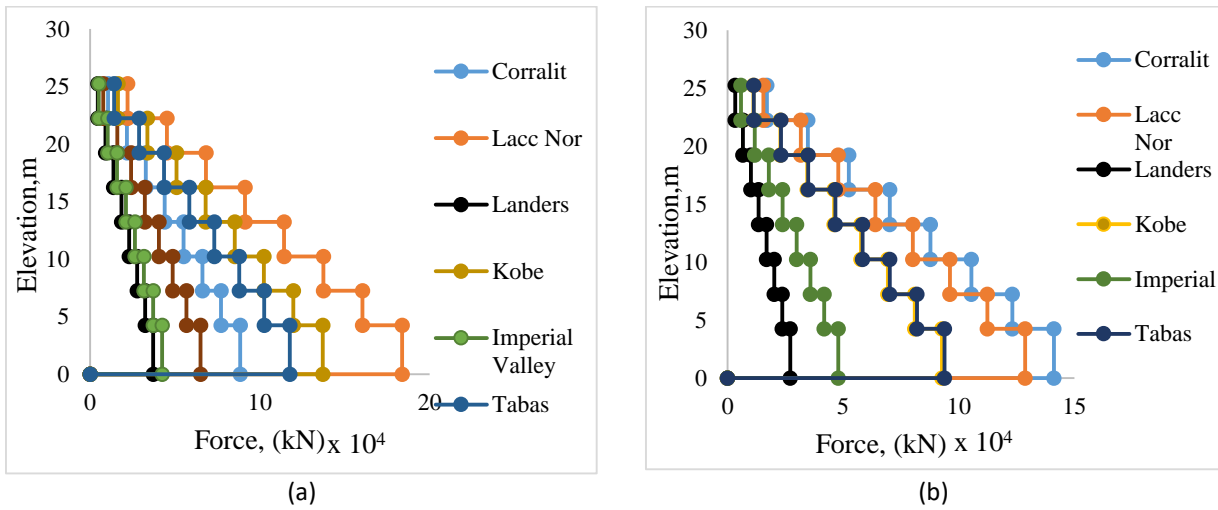


Fig. 7: Story shear under different earthquake GMs (a) X- Direction; (b) Y-Direction.

Table 6: Shear force distribution in column and wall

Story	Wall	Load cases	Wall Shear (kN)	Column	Column Shear (kN)	% Shear by Columns	% Shear by Core Wall
Story1	P3	Corralit max	84215	All	1638	1.91	98.09
Story1	P3	Corralit max	84215		1639	1.91	98.09
Story1	P3	Lacc_Nor max	189115		3543	1.84	98.16
Story1	P3	Lacc_Nor max	189115		3546	1.84	98.16
Story1	P3	Kobe max	134508		2610	1.90	98.10
Story1	P3	Kobe max	134508		2613	1.91	98.09
Story1	P3	Tabas max	104577		2104	1.97	98.03
Story1	P3	Tabas max	104578		2106	1.97	98.03
Story1	P3	Landers max	73659		1566	2.08	97.92
Story1	P3	Landers max	73659		1568	2.08	97.92
Story1	P3	Imperial Valley max	39621		962	2.37	97.63
Story1	P3	Imperial Valley max	39621		962	2.37	97.63

The absolute maximum displacement of the structure under different ground motions is presented in Fig. 8. It is observed from the figure that the lateral displacement is maximum at the roof level for all types of models. Lateral

displacement is minimum at base level and maximum at roof level thus as the storey level increases lateral displacement is also observed to be increased.

The storey drifts of the structure for the ground motions in both X and Y directions are presented in Fig. 9. The inter-story drift in X direction is observed at the 5th storey level which is at the 3rd storey level for Y direction. Inter-drift ratio increased with increase in story level up to the largest inter-story drift for both direction and thereafter reverse trend are observed for all earthquake ground motions. The difference in behavior among different earthquakes is further appreciated by referring to Fig. 9, depicting the base shear, lateral displacement and inter-storey drifts.

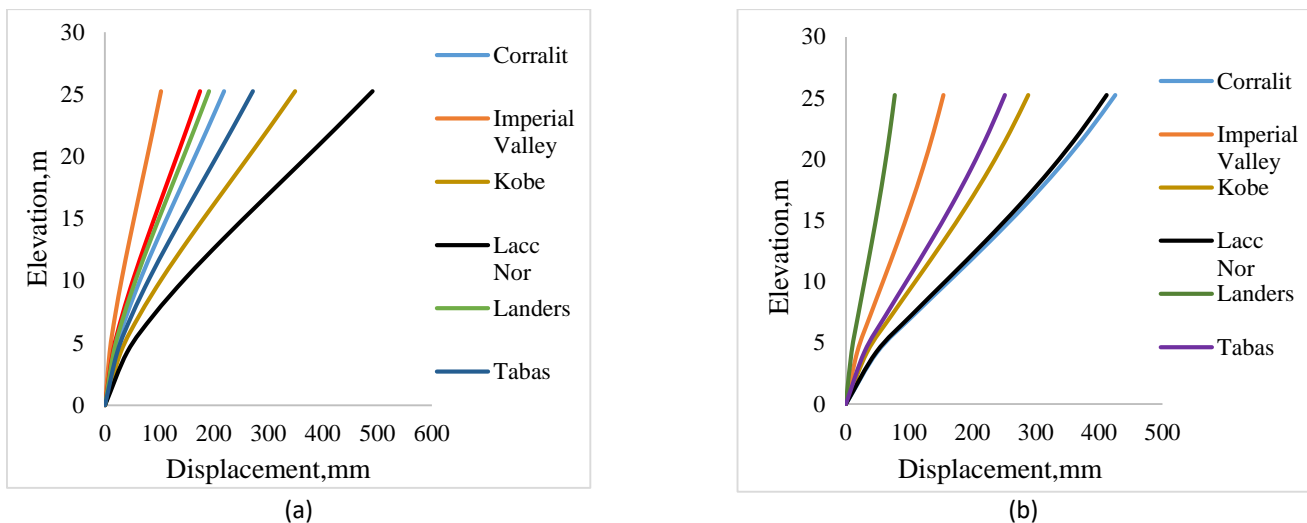


Fig. 8: Maximum story displacements: (a) X-Direction; and (b) Y-Direction.

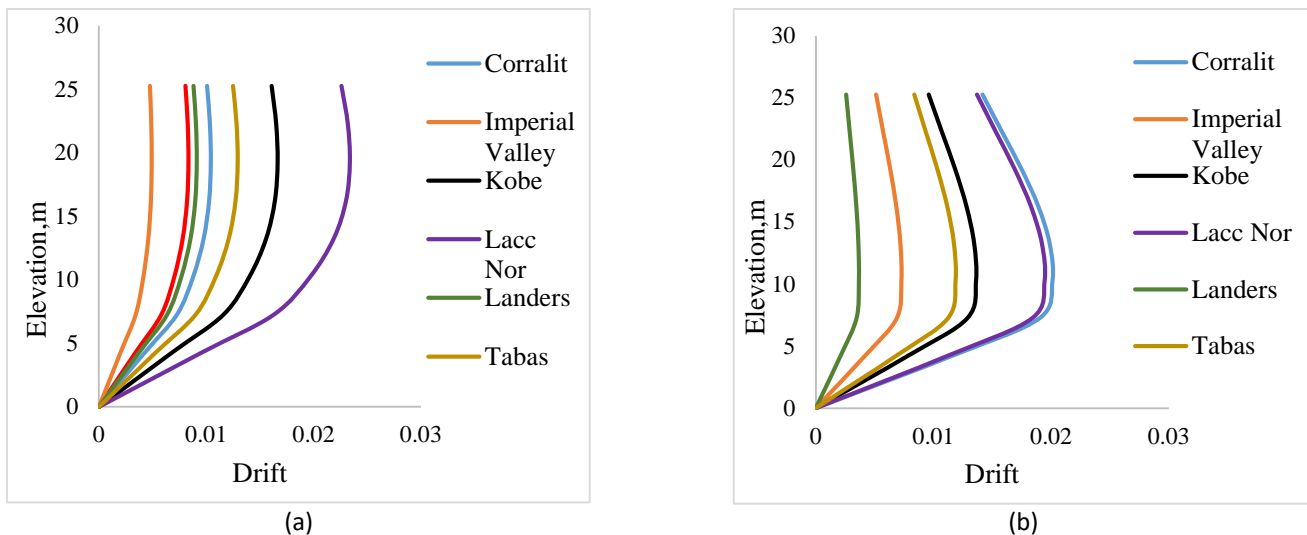


Fig. 9: Maximum story drifts: (a) X-Direction; and (b) Y-Direction.

Non-linear responses of frame hinge i.e. column hinges are shown in figure 10. The column 1 represents the corner column and column 5 presents other typical exterior column. It is observed from the figure that the corner column shows inelastic response in only two ground motions (Corralit and Tabas). On the other hand, all other exterior columns show

inelastic responses for all six set of earthquakes. Maximum positive and negative chord rotations are observed for Lacc_Nor and Kobe earthquake respectively. The resulting maximum moment is nearly 1000kN-m with a rotation of 2×10^{-3} rad.

Hysteretic responses of wall hinge at the ground floor level are presented in Fig.11. The colors of different ground motions clearly highlight their hysteretic response in terms of moment rotation responses. The figure shows that the wall hinge at the first storey level reaches yield to ultimate level. Response of different hinges are different due to different geometric condition, locations and orientation. The amount of moment carrying capacity of the wall also depends on the sizes of the wall and their direction with respect to the ground motions.

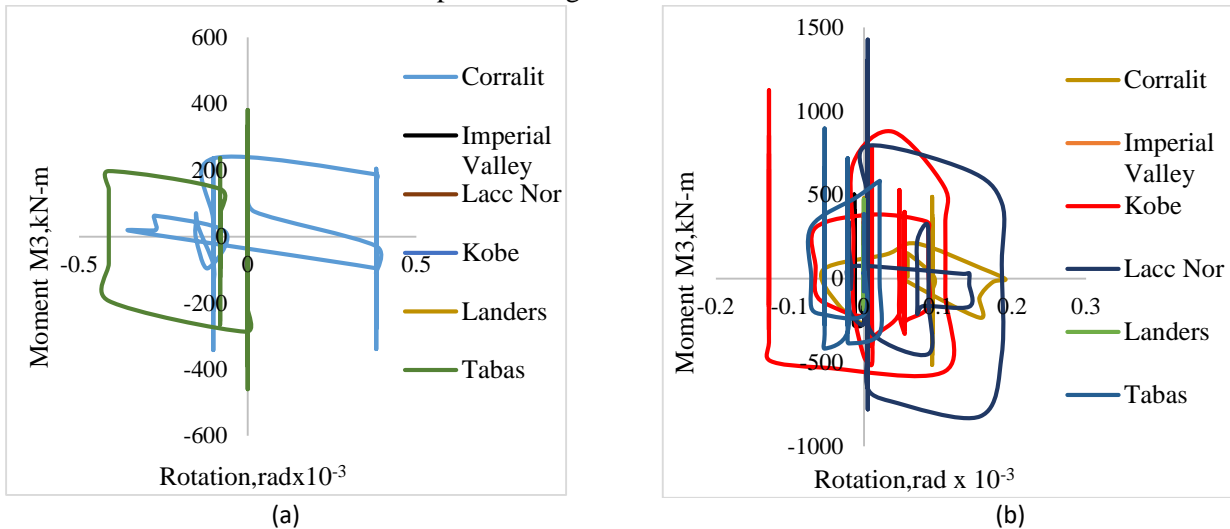


Fig. 10: Column hinge response under time history functions (a) Column 1; and (b) Column 5.

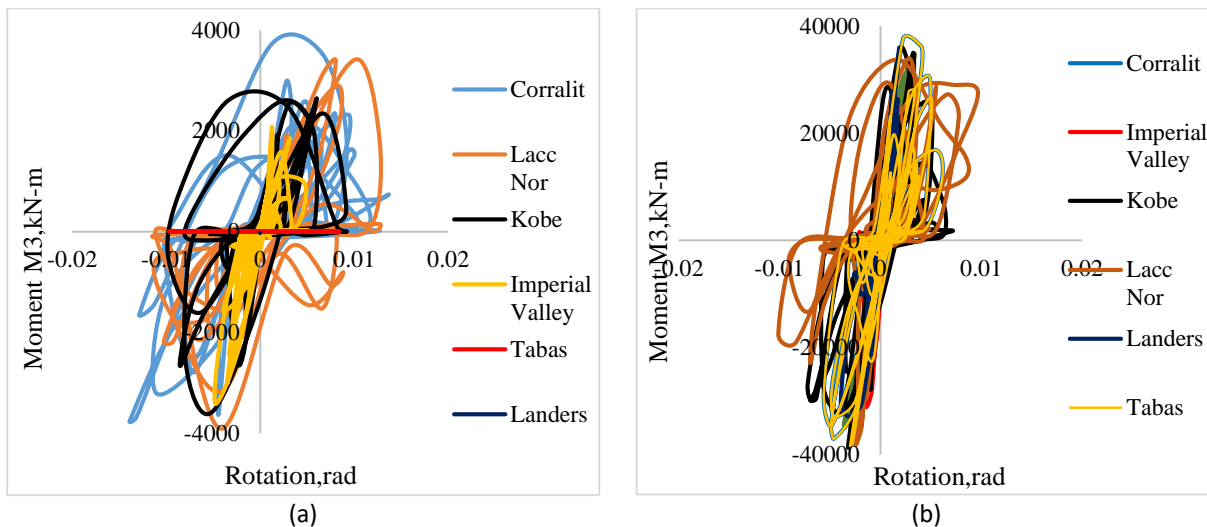


Fig. 11: Wall hinge response under time history functions: (a) Wall label 4; and (b) Wall label 5.

The hysteretic response of concrete and steel fibers are presented in Fig. 12(a) and 12(b), respectively. It can be seen from the Fig. 12(a) that concrete fiber inside the core shear wall is primarily resting in the compression zone and also in some tension zone following the actual backbone curve of the concrete. Maximum compressive stress (35 MPa) was reached in all ground motions whereas maximum strain is 0.006 was observed in Lacc_Nor and Kobe GMs. The hysteretic response of the steel fiber inside the shear wall can be observed in the Fig. 12(b). The figure shows that once the steel fiber reaches

the yield strength level it goes to inelastic zone of the fiber and plastic deformation occurs. The maximum plastic deformation of the rebar was observed for Lacc_Nor ground motions. It is also important to highlight that the steel fiber forms the backbone curve as it progresses to the plastic deformation. Detail fiber stress, strain and states of fibers of a wall at ground floor level is presented in Table 7. For fiber hinge states of the shear wall, most of hinges are in the range of A to IO state and some are in IO to LS state. For example, fiber number 1 and 7 reach the IO to LS level and all other remain in A to IO level. The result shows that the fiber hinge state of the individual fiber provides the building performance and efficiency level of the structure.

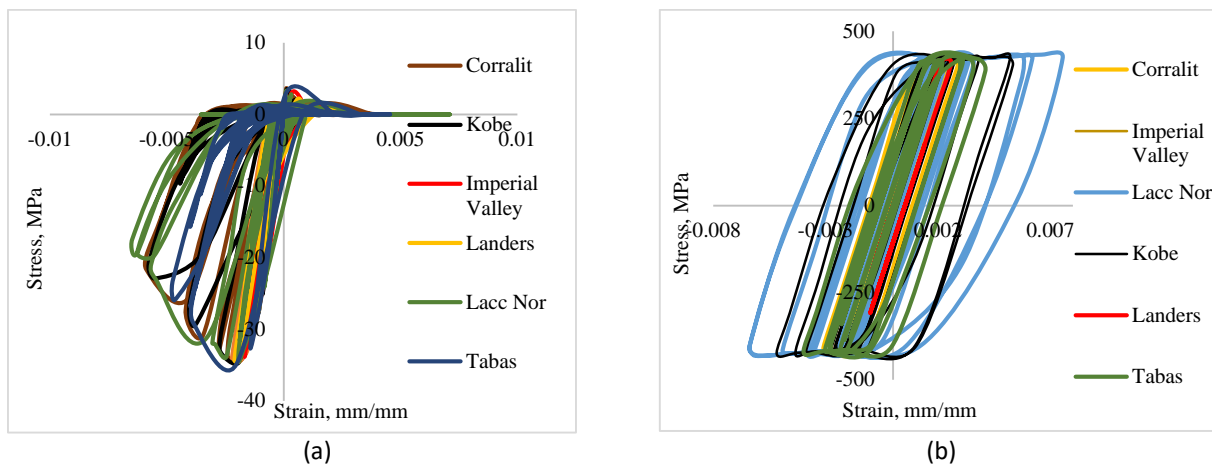


Fig. 12: Fiber responses (a) Fiber 1 (concrete) and (b) Fiber 13 (Steel).

Table 7: Fiber Hinge States (Fiber Status)

Story	Wall	Load cases	Fiber no.	Fiber area	Stress (MPa)	Strain	Fiber state	Fiber status	Fiber material
Story1	W4	Lacc_Nor max	1	415.6	3.33	0.0071	A to B	A to IO	C35/45
Story1	W4	Lacc_Nor max	7	415.6	2.86	0.0076	A to B	A to IO	C35/45
Story1	W4	Lacc_Nor max	8	2.1	433.47	0.0069	B to C	A to IO	A615Gr60
Story1	W4	Lacc_Nor max	13	2.1	432.27	0.0075	B to C	A to IO	A615Gr60
Story1	W4	Lacc_Nor min	1	415.6	-34.46	-0.0064	>E	IO to LS	C35/45
Story1	W4	Lacc_Nor min	7	415.6	-34.38	-0.0065	>E	IO to LS	C35/45
Story1	W4	Lacc_Nor min	8	2.1	-430.26	-0.0062	B to C	A to IO	A615Gr60
Story1	W4	Lacc_Nor min	13	2.1	-430.4	-0.0063	B to C	A to IO	A615Gr60
Story1	W5	Lacc_Nor max	1	748.1	2.99	0.00908	A to B	A to IO	C35/45
Story1	W5	Lacc_Nor max	6	1496.3	3.15	0.00438	A to B	A to IO	C35/45

Story1	W5	Lacc_Nor max	12	3.8	439.62	0.00878	B to C	A to IO	A615Gr60
Story1	W5	Lacc_Nor max	17	3.8	422.49	0.00422	B to C	A to IO	A615Gr60
Story1	W5	Lacc_Nor min	1	748.1	-34.84	-0.0089	>E	IO to LS	C35/45
Story1	W5	Lacc_Nor min	6	1496.3	-33.38	-0.0037	B to C	A to IO	C35/45
Story1	W5	Lacc_Nor min	12	3.8	-437.7	-0.0085	B to C	A to IO	A615Gr60
Story1	W5	Lacc_Nor min	17	3.8	-418.86	-0.0035	B to C	A to IO	A615Gr60

4. Conclusion

In this study, an 8 storey RC structure having flat slab system and core shear wall has been deeply analyzed using displacement-based analysis and design procedure. Non-linear fiber hinge models are adopted to determine the response and role of core shear in seismic force resistance of flat slab system. The analysis has been run for six pairs of earthquake ground motions. The key finding of the non-linear dynamic analysis is briefly as follows.

- The non-linear analysis revealed that the inelastic response of the hinges is higher in the core shear wall than that of the gravity columns. The resulting base shear for all ground motions primarily shows that almost 98% of the total base shear is taken by the core shear wall where the remaining 2% is taken by the all column sections.
- The storey displacement of the structure is highly non-linear and maximum is observed at the roof of the structures for all ground motions. The storey drift is also observed non-linear along the height of the building. The maximum storey drift is observed at the 5th storey level in X direction and 3rd storey level at the Y direction.
- Column hinge response shows that corner columns experience plastic rotation only for two ground motions (Lacc_Nor and Kobe) whereas other exterior columns reach through the inelastic behaviors for all ground motions. Maximum chord rotation is observed to be 2×10^{-4} which is well below the ultimate rotation.
- Maximum chord rotation and moment are observed at the ground floor level. Wall hinge shows that the hysteretic responses of wall hinge perpendicular to the direction of GMs are flatter than those parallel to the GMs. Wall hinges reaches to a chord rotation of 0.012 rad for Corralit and Kobe earthquake. Fiber hinge response also shows that few fibers of W4 and W5 reach to IO to LS state whereas most of the hinges are in A to IO state.
- This study also determines states of hinges from the hysteretic response of individual concrete and steel fibers. The result shows that both concrete and steel fiber show the inelastic response for all six GMs and forms the backbone curve as it progresses through the larger strain. The maximum residual strain for concrete and steel are 0.003 and 0.006 for concrete and steel respectively, which were observed for Kobe and Lacc_Nor ground motions.

It can be concluded that this displacement-based approach is capable to determine the actual response of complex structures or irregular geometry subjected to any earthquake ground motions. The stress and strain levels of each structural component can be understood more accurately and hence the structural design can be performed more accurately.

References

- [1] P. Chandurkar and D. Pajgade, "Seismic analysis of RCC building with and without shear wall," *International journal of modern engineering research*, vol. 3, no. 3, pp. 1805-1810, 2013.
- [2] M. W. White and J. D. Dolan, "Nonlinear shear-wall analysis," *Journal of Structural Engineering*, vol. 121, no. 11, pp. 1629-1635, 1995.
- [3] T. Tabassum and K. S. Ahmed, "Improving lateral load bearing capacity of RC buildings using non-linear dampers," *Journal of Civil Engineering*, vol. 46, no. 1, pp. 31-40, 2018.

- [4] K. S. Ahmed, A. Tasnim, and A. Farzana, "Seismic Performance Investigation of Base Isolation System for Typical Residential Building in Bangladesh," *MIST International Journal of Science and Technology*, vol. 4, no. 1, 2016.
- [5] T. Tabassum and K. Ahmed, "Seismic Performance of Damper Installed In High-Rise Steel Building In Bangladesh," *Journal of Civil Engineering, Science and Technology*, vol. 9, no. 1, pp. 1-12, 2018.
- [6] J. Moehle, "Displacement-based design of RC structures subjected to earthquakes," *Earthquake spectra*, vol. 8, no. 3, pp. 403-428, 1992.
- [7] X. Zeng, X. Lu, T. Yang, and Z. Xu, "Application of the FEMA-P58 methodology for regional earthquake loss prediction," *Natural Hazards*, vol. 83, no. 1, pp. 177-192, 2016.
- [8] R. Mahmud and K. S. Ahmed, "Interface dependency of reinforced concrete jacketing for column strengthening," *Proceedings of the Institution of Civil Engineers–Structures and Buildings*, vol. 173, no. 1, pp. 31-41, 2020.
- [9] K. S. Ahmed, M. Shahjalal, T. A. Siddique, and A. K. Keng, "Bond strength of post-installed high strength deformed rebar in concrete," *Case Studies in Construction Materials*, p. e00581, 2021.
- [10] K. Islam, A. M. Billah, M. M. I. Chowdhury, and K. S. Ahmed, "Exploratory study on bond behavior of plain and sand coated stainless steel rebars in concrete," *Structures*, vol. 27, pp. 2365-2378, 2020.
- [11] "Computer and Structures Inc. ," "ETABS Nonlinear Version 16.2", vol. California, USA.
- [12] ASCE, "Minimum design loads for buildings and other structures," 2013: American Society of Civil Engineers.
- [13] F. Flores, F. Charney, and D. Lopez-Garcia, "The influence of gravity column continuity on the seismic performance of special steel moment frame structures," *Journal of Constructional Steel Research*, vol. 118, pp. 217-230, 2016.